Journal of Mechanical Research and Application (JMRA),Vol. 13 No.4, 1402(2023),48-54

Effect of Al concentration in microstructure and mechanical properties of TiAlN thin films

M. Manouchehrian

Department of Physics, South Tehran Branch, Islamic Azad University, Tehran, Iran

Email:mehdi_manoochehrian@yahoo.com

Abstract

In this work, a series of (Ti, Al) N coatings with different Al contents were deposited on 304 stainless steel substrates by Hollow Cathode Discharge (HCD) method. The coatings were grown on 304 stainless steel substrates a T=400 ◦C. The coating were characterized using energy dispersive X-ray spectroscopy (EDX), X-ray diffraction (XRD), atomic force microscopy (AFM) and microhardness test. TiN phase to (Ti, Al) N phase and then to AlN phase with increasing Al concentration in the solid solution. It was found that with increasing Al concentration the hardness of the coatings initially increased up to a maximum value of about 30 GPa at around 32 at.% of Al and then the coating hardness decreased rapidly with further increase of Al content (Al > 32 at.%).

Keywords: coating, XRD, AFM, hardness

Introduction

In the past two decades, coatings of the (Ti, Al)N ternary system have been used extensively in surface coating application due to their excellent material properties including superior hardness [1], low wear [2,3], corrosion resistance [4],and oxidation resistance at high temperature [5,6]. In recent years, (Ti, Al) N coatings have been widely developed in many application fields such as cutting and forming tools [7,8], semiconductor devices [9] and optical instruments [10]. The incorporation of Al into the face center cubic (fcc) structure of TiN results in the formation of a metastable ternary solid solution (Ti, Al)N whose properties depend on the method and

parameters used for their preparation. In this work, we propose to study the effect of Al incorporation at different concentrations in TiN coating tacking into consideration the microstructure, hardness and corrosive behavior of the coatings.

Experimental Details

Deposition of (Ti, Al) N coating on stainless steel (SS) 304, was carried out in active N_2 ambient using hollow cathode discharge (HCD) gun model DLKD-1800 with 15 kW power as described in [11]. The substrates were cut into 10 mm × 10 mm slabs then they were cleaned with acetone and ethanol in an ultrasonic bath for 15 min. The vacuum chamber base pressure was 3×10^{-3} Pa. Granules of pure titanium (99.8%) mixed with different contents of pure Al (99.8%) was used as coating materials. Prior to deposition, substrates were bombarded by argon ions produced in electric discharge chamber for 30 min. To end-process of surface cleaning. The working pressure was 3×10^{-3} Pa with introducing the reactant gas of nitrogen. The bias voltage and substrate temperature were fixed at −60 V and 673 K respectively during the deposition. The phase and crystalline structure of the coating were characterized by X- ray diffraction (XRD) using a Philips-PW 1800 with Cu (K_α) radiation (λ=0.15406) which was operated at 40 kV and 30 mA. The scanning was conducted from 20° to 60° at step size 0.02° and 1 s per step. The morphology and chemical composition of the coatings were determined by scanning microscope electron (SEM) using a Philips-XL300 and energy dispersive X-ray (EDX) with an accelerating voltage 25 Kv. The topography and roughness of the coatings were investigated using an atomic force microscope (AUTO PROBE- CP) in contact mode. The microhardness tests were performed using a MVK-H21 with a Vickers indenter and an indentation load of 100 mN. The hardness value is a result of at least five indentation tests for each sample.

Results and Discussion

Examples of EDX spectrum for (Ti, Al) N coatings are given in figure 1. The content of Al and Ti in deposited films determined by EDX analyses are summarized in table 1 by taking into account that the nitrogen content in all samples is close to 50 at.%. The peak of Fe in the figure is related to the substrate.

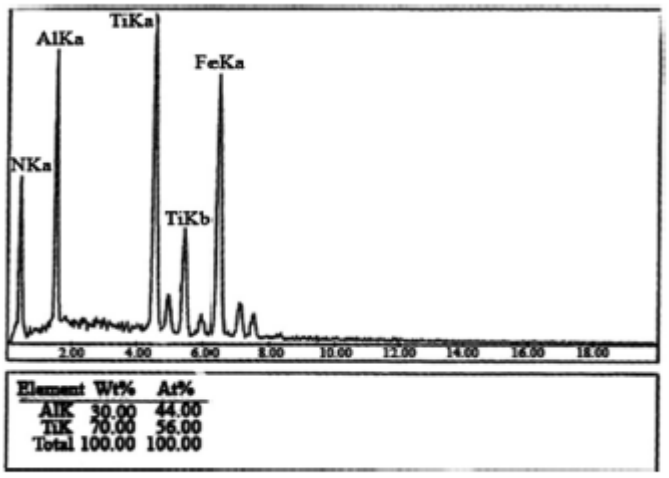

Fig. 1 Example of EDX spectrum for (Ti, Al) N coatings.

Table 1 Ti and Al atomic composition of (Ti, Al) N coatings measured by EDX area analyses.

Sample	Ti (at.%)	Al (at.%)
C_1	100	0
C_2	92	8
C_3	84	16
C_4	68	32
C_5	56	44
C_6	50	50
C_7	10	90

Figure 2 shows XRD patterns of samples with different Al contents. In all XRD patterns the peaks at $2\theta = 43.57^{\circ}$, $2\theta = 44.63^{\circ}$ and $2\theta = 50.70^{\circ}$ are related to 304 stainless steel substrate (ref. code 00-033-0397). For sample C1, in addition to three peaks mentioned above, the TiN(111) and TiN(200) peaks with B1-NaCl structure are observed at 35.96° and 42.08° respectively (standard JCPDS No: 87-0631). For samples C2 − C5, with Al content 8–44 at.% a new phase corresponding to (Ti, Al) N (111) and (Ti, Al) N (200) with B1-NaCl structure[11] is formed. With increasing Al concentration in film (50 at.%), a mixture consisting of solid solution and hexagonal wurtzite AlN are observed. For Al content 90 at.%, it can be seen that only hexagonal AlN is present in the deposited film. This observation is in consistent with that of reported by [12] in which is predicted a content of Al the wurtzite phase is predicted to be energetically favorable. Under our experimental temperature, the metastable solid solution (Ti, Al) N with B1-NaCl structure is more stable for Al content lower than 68 at.% and wurtzite structure is more stable for Al content larger than 68 at.% [13]. It is obvious from figure 2 that the TiN peaks slightly shift towards the higher Bragg angle with increasing the Al concentration. The increase of 2θ is probably related to the substitution of Ti atoms by Al atoms and the formation of (Ti, Al) N phase. Knowing

that the atomic radius of Al (0.143 nm) is smaller than that of Ti atom (0.146 nm); one can expect a decrease of lattice parameter (i.e., an increase of Bragg angle) after substitution. On the other hand, the incorporation of Al atoms in the TiN film structure can probably increase the strain in the film leading to a displacement of the Bragg angle towards the higher values. With Al content of 50 at.%, an over-saturation of Al concentration in the film may occur imposing thermodynamically a partial phase transformation of (Ti, Al) N to AlN. Further increase of Al concentration in the film results in the film a decrease of the (Ti, Al) N peak intensity in favor of AlN phase formation. In fact, this transformation continues until the (Ti, Al) N phase disappears at Al 90 at.% and only AlN phase is present as shown in figure 2. In theses conditions, the Ti atoms act as impurities in the novel phase.

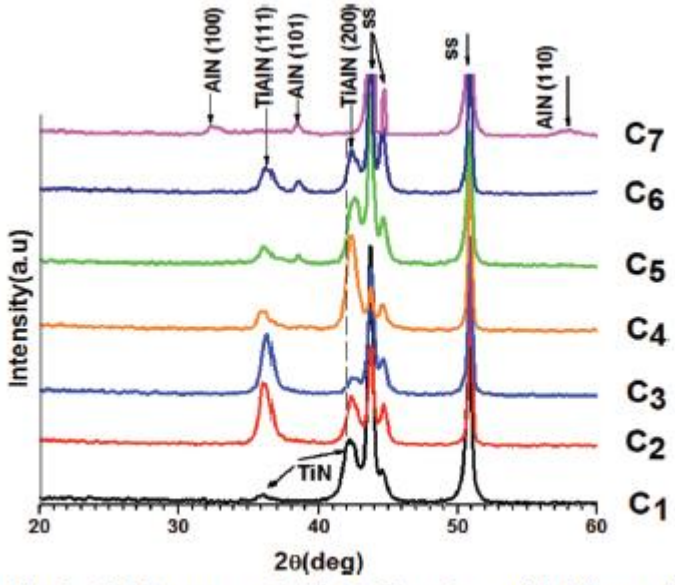

Fig. 2 XRD patterns of (Ti, Al) N coatings with different Al contents.

The effects of Al concentration on the microstructure of different coatings are shown in figure 3. The surface topography of the coatings is performed using height AFM for a scanned area of 2 μm×2 μm. The images reveal that the grain size and shape on the c oating surface vary with coating composition. The TiN coating (figure 3a corresponding to sample C_1) shows a granular and dom elike structure in which the round grains with the nearly equal size are distributed with distance to one another on the surface. With the increase of Al content up to 50 at.% in the film, the grains join together forming a maize-seed like structure (figure 3b). Further increase of Al content in the coatings (50 at.%) leads to the formation of some hillock structure besides the domelike stru cture and the grains are different in size as shown in figure 3c. In sample C_7 (figure 3d) where AlN single phase is present, the dom elike structure of the coating fully changes to hillock structure. From the observation of figure 3b it becomesclear that the mentione

d maize-seed-like structure is actually an epitaxial Ti-rich solid solution coatings. Grain orientation along a definite crystallographic direction is eye-striking in this image, giving rise to subparallel lineal discontinuities. All the remaining images displayed in figure 3 show randomly oriented coatings. Figure 4 shows the average and root mean square (rms) roughness of coatings as a function of Al concentration. The surface roughness of different samples nearly remains constant up to 50 at.% within the accuracy of measurement (20%), but dramatically increases above this value probably because of the formation of AlN phase with hexagonal structure and increase of grain size as shown in 2D images of figure 3. The acquired roughness data remarkably support our above observation from height AFM images, where two groups can be clearly defined, separating solid solution members from mixtures dominated by hexagonal AlN. Sample C_5 is clearly still dominated by the presence of an Al-rich solid solution phase, retaining a low level of roughness.

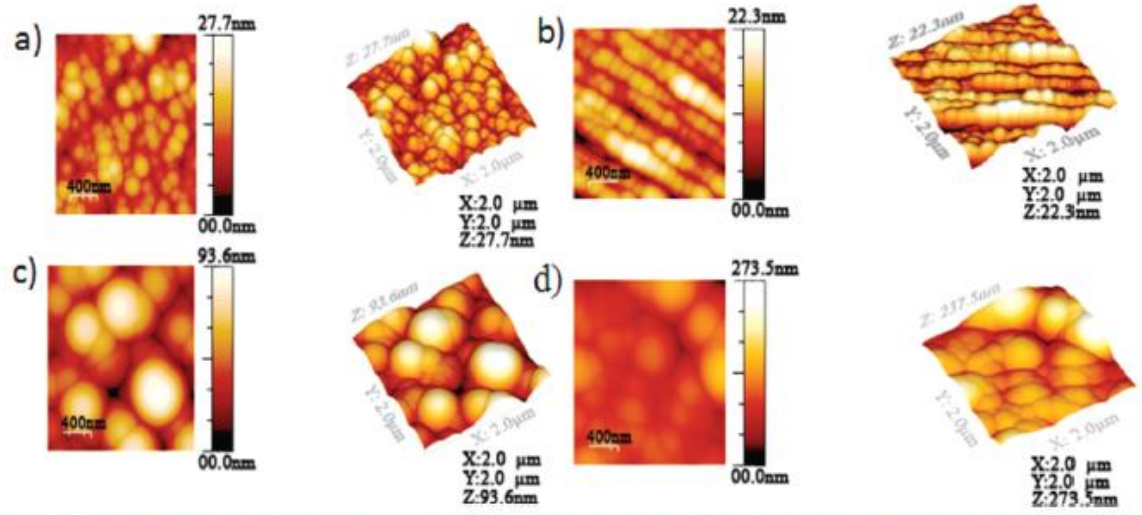

Fig. 3 2D and corresponding 3D height AFM images of (Ti, Al) N coatings with different Al content: (a) sample c_1, (b) sample c_2, (c) sample c_6 and (d) sample c_7.

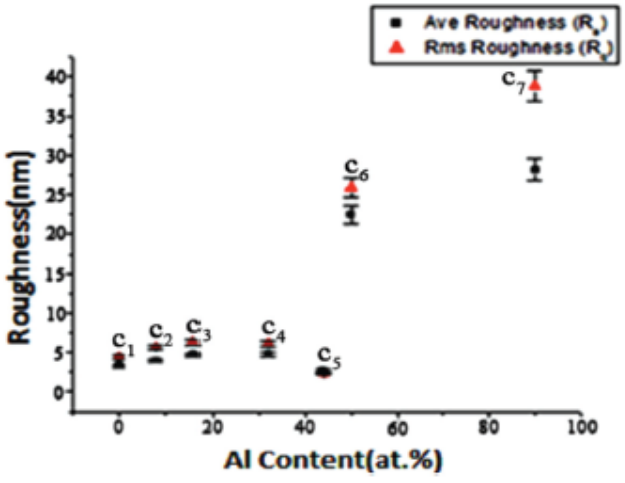

Fig. 4 The variation of average (R_a) and root mean square (R_q) roughness of deposited (Ti, Al) N coatings as a function of Al content.

Figure 5 shows the microhardness of the coatings as a function of Al concentration. The coatings exhibit a gradual increase of hardness with increase of Al concentration in the region of 0-32 at.%. The highest hardness occurs in Al content of 32 at.% with maximum value of 30 GPa. Above this concentration an abrupt decrease of hardness is caused. The increase of hardness is due to the incorporation of Al atoms in the TiN crystalline structure which avoid the operation of different slip systems in the crystal structure and microscopic dislocation motions and plastic deformation by causing crystal lattice distortion. The decrease in hardness is probably due to softening of the coatings by inclusion of the AlN phase [15], and also to the phase and structure tran sformations from fcc to wurtzite [16]. Moreover, the increase of surface roughness as shown in figure 4 could decrease the hardness by reducing the effective contact area.

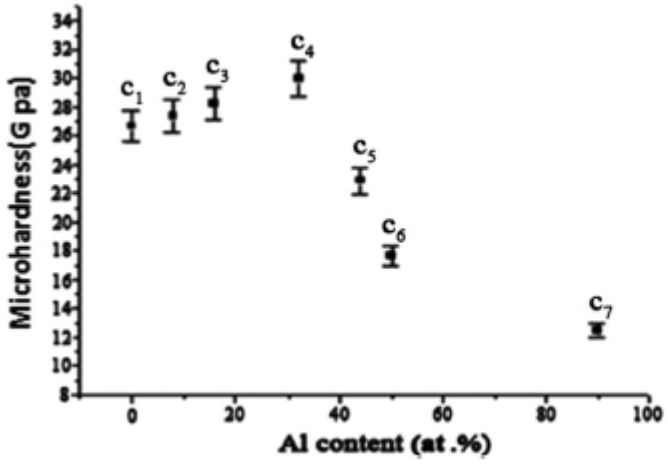

Fig. 5 Microhardness of the as-deposited (Ti, Al) N coatings as a function of Al content.

Conclusion

TiN coatings deposited on AISI 304 show a remarkable improvement in hardness with substitutional incorporation of Al atoms in the coatings due to the formation of alloy nitride (Ti, Al) N phase. We have demonstrated that the hardness is mainly controlled by Al content in TiN films. The coatings exhibited a maximum hardness of 30 GPa.

References

[1] C. T. Huang, J. G. Duh, and J. Mater, Sci. Lett. **16**, 59 (1997).

[2] J. D. Bressan, R. Hesse, and Jr. EM. Silva, Wear. **250**, 561 (2001).

[3] S. G. Harris, E. D. Doyle, A. C. Vlasveld, J. Audy, and D. Quick, Wear. **254**, 723 (2003).

[4] S. H. Ahn, J. H. yoo, Y. S. Choi, J. G. kim, and J. G. Han, Surf. Coat. Technol. **162**, 212 (2003).

[5] D. Mcintyre, J. E. Green, G. Hakansson, J. E. Sundgren, and W. D. Munz, J. Appl. Phys. **67**, 1542 (1990).

[6] C. T. Huang and J. G. Duh, Surf. Coat. Technol. **81**, 164 (1996).

[7] M. C. kang, I. W. park, and K. H. kim, Surf. Coat. Technol. **163–164,** 734 (2003).

[8] C. T. Huang and J. G. Duh, Surf. Coat. Technol. **71**, 259 (1995).

[9] S. D. Kim, I. S. Hwang, J. K. Rhee, T. H. Cha, and H. D. Kim, Electrochem. Solid-State. Lett. **4**, G7 (2001).

[10] M. Hock, E. Schaffer, W. Doll, and G. kleer, Surf. Coat. Technol. **163–164**, 689 (2003).

[11] P. Kuppusami, C. Sanjeeviraja, and M. Jayachandran, Cryst. Res. Technol. **43**, 1067 (2008)

[12] D. Holec, R. Rachbauer, Li. Chen, L. Wang, D. Luef, and Paul H. Mayrhofer, Surf. Coat. Technol. (2011), doi: 10.1016/J.SURFCOAT.2011.11020.

[13] R. F. Zhang and S. Veprek, Mater. Sci. Eng. A. **448**, 111 (2007).

[14] J. T. Chen, J. Wang, F. Zhang, G. A. Zhang, X. Y. Fan, Z. G. Wu, and P. X. Yan, J. Alloys Compd. **472**, 91 (2009).

[15] X. Li, C. Li, Y. Zhang, H. Tang, G. Li, and C. Mo, Appl. Surf. Sci. **256**, 4272 (2010).

[16] P. H. Mayrhofer, A. H¨orling, L. Karlsson, J. Sj¨ol´en, T. Larsson, C. Mitterer, and L. Hultman, Appl. Physics. Lett. **83**, 2049 (2003).